Role of the Near Earth Plasmasheet at Substorms

A. Roux, S. Perraut, A. Morane, P. Robert, A. Korth, G. Kremser, A. Pederson, R. Pellinen, and Z.Y. Pu

Recent observations performed onboard GEOS-2 and AMPTE CCE and IRM have renewed the interest for the role played by the inner plasmasheet at substorms. GEOS data are used to show that (i) electron injection at breakup is dispersionless and is therefore due to a local process, (ii) strong earthward gradients in the flux of energetic ions are observed prior to breakup; after breakup, the direction of this gradient oscillates, and (iii) oscillations are also identified in electric and magnetic field data; they correspond to an azymuthallypropagating wave. These results are shown to be consistent with a ballooning instability developing in the highly-stressed magnetic geometry that builds up in the Central Plasma Sheet (CPS) prior to substorms. As it grows, this instability drives a system of transient field-aligned currents, hence leading to the partial cancellation of the tail current. This results in an increase of the H component of the magnetic field (the dipolarization) and to the corresponding induced electric field resulting in particle injection. Comparison with the ground-based ASC (All-Sky Camera) suggests that the surges observed simultaneously on the ground are the image of this instability drawn onto the upper atmosphere by precipitating electrons. According to this interpretation, the northward expansion of the auroral arcs reflects the radial expansion of the region where the ballooning instability develops. The validity of this interpretation is checked against data from AMPTE CCE and IRM and from ISEE-1,2.

1. INTRODUCTION

On All-Sky Camera (ASC) pictures, the substorm breakup is usually characterized by a rapid brightening and development of a surge, which later propagates or expands to the West. The Westward Travelling Surge (WTS) is formed at the poleward edge of the diffuse auroral region, at magnetic latitudes in the range 65 to 70°. While the southern edge of the region where bright auroras develop is essentially unchanged, the arcs and bulges expand to the

West, to the East and, at a slower velocity, to the North. This asymmetric expansion is very clear on images from DE1 and Viking. About 30 mn after breakup, various arcs cover from ~ 65-70° to 75-80°.

A strong upward field-aligned current, associated with precipitating electrons, flows near the leading edge of the WTS [Opgenoorth et al., 1983] and the signature of reverse currents, flowing towards the Earth, has also been identified east and west of the WTS [Kozelova and Lyatskiy, 1984]. Then, a system of field-aligned currents develops, as the WTS is formed. The relationship between the formation of the surge and the field-aligned current system is discussed in the present work.

Following *Dungey* [1961], several authors have discussed the possible connection between substorm development and the formation of an X point or line in the central part of the geomagnetic tail. According to a widely spread scenario, the thinning of the CPS produces a very small B_Z component, which favours the development of tearing modes. In the collisionless CPS plasma, however, the development of the tearing mode instability is not granted: *Lembège and*

³Department of Physics, University of Oulu, Oulu, Finland ⁴ESTEC/SSD, Noordwijk, The Netherlands

Finnish Meteorological Institut, Helsinki, Finland

Magnetospheric Substorms Geophysical Monograph 64 Copyright 1991 American Geophysical Union

¹CNET/CRPE/CNRS, Issy-les-Moulineaux-Cedex, France ²Max-Planck Institut fur Aeronomie, Katlenburg-Lindau, Germany

Department of Geophysics, Beijing University, Beijing, P.R.C.

Pellat [1982] have shown, indeed, that even a very small B_z component can stabilize the tearing modes. Should B_z be locally small enough to allow the tearing instability to develop, then B_z would grow, anyhow, as a consequence of the instability. The saturation level of the tearing mode instability is therefore expected to be quite small, hence raising questions as to its importance in the dynamics of the geomagnetic tail.

Substorm onset in the near Earth plasmasheet at the geosynchronous orbit is characterized by a reconfiguration of the magnetic field, initially tail-like, towards a more dipole-like configuration [Sauvaud and Winckler, 1980] and by an injection of energetic particles [Mauk and McIlwain, 1974]. This magnetic reconfiguration is associated to a reduction, at least locally, of the cross tail current. McPherron et al. [1973] interpreted this reduction in terms of a current wedge that diverts a fraction of the tail current into the ionosphere, via field-aligned currents. Injection of energetic particles is often dispersionless, hence it must be achieved by a local acceleration process. Mauk and Meng (1987) suggest that an induced electric field, associated with the reconfiguration of the magnetic field, does produce the required acceleration. In the present paper, we show that the dipolarization, the current wedge and the injection are due to a single cause: the development of the ballooning instability in the near Earth plasmasheet.

This work is based on the interpretation of data from the geostationary satellite GEOS-2. These data are presented and discussed in Section 2. Experimental evidence for the development of a ballooning instability is given in Section 3. The theoretical framework of the ballooning instability is discussed in Section 4. In Section 5, the consequences of the development of the ballooning instability are discussed in the context of ISEE and AMPTE measurements performed beyond the geostationary orbit.

2. SUBSTORMS AT THE GEOSTATIONARY ORBIT

The present section is mainly based on data registered in the near Earth plasmasheet, close to the geographic equator, by the ESA/GEOS-2 spaceraft. This section is a summary of a work by *Roux et al.* (1991), who studied in detail an isolated dispersionless substorm that took place on January 25, 1979. About 20 similar isolated dispersionless events, observed on GEOS-2, are analysed in a companion paper by *Korth et al.* [1991, this issue].

Full advantage is taken of the stationary position of GEOS-2, to make a comparison with ground-based data. On January 25, 1979, ground-based magnetometers at Kiruna and riometers at Kilpisjärvi show the typical signature of an isolated substorm [see *Roux et al.*, 1991, for more details].

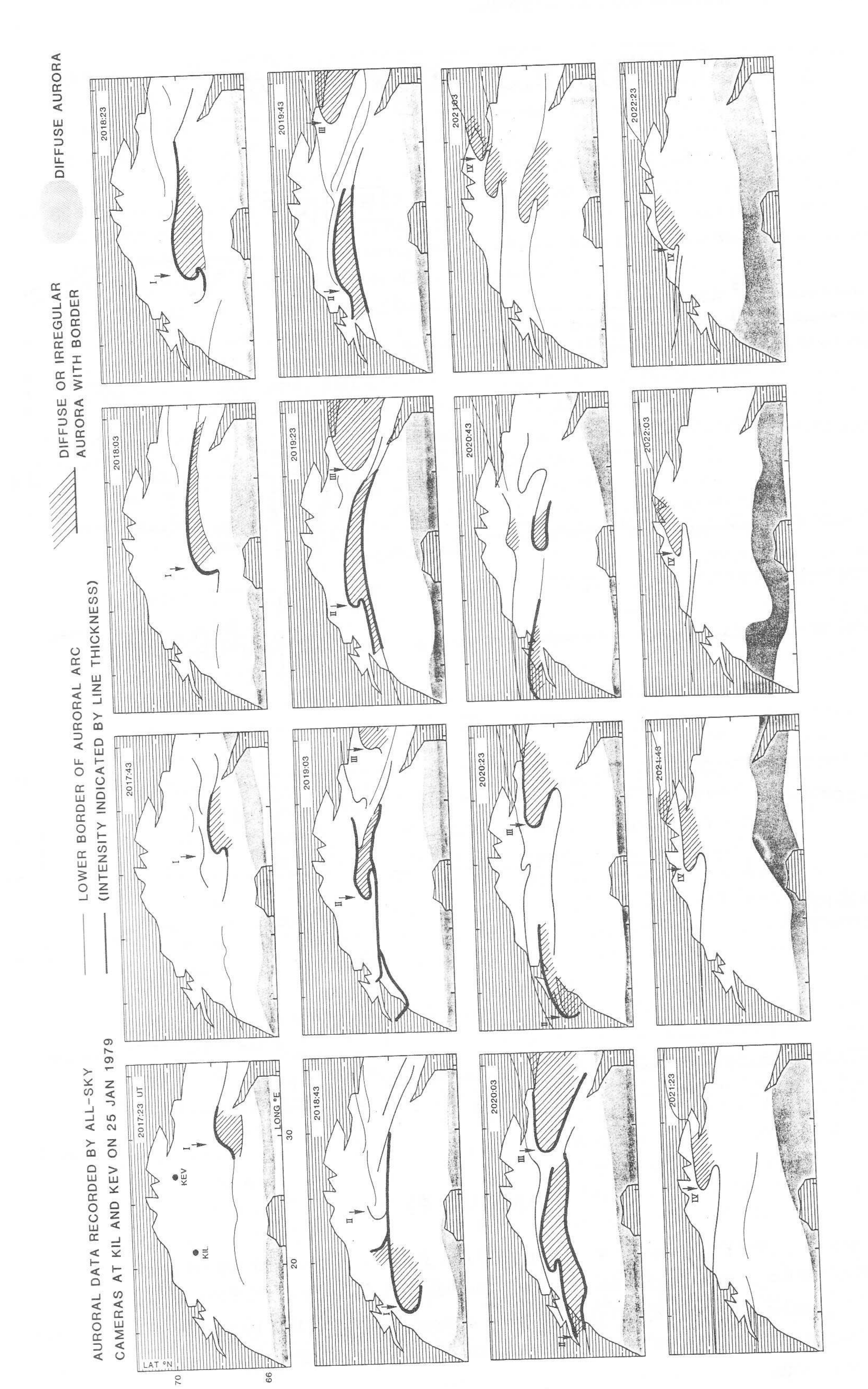
For future discussions, the signature of the breakup on ASC's is important to describe. Figure 1 shows defolded images built from pictures gathered simultaneously by two ASC's, one at Kevo (69.8° N, 29.0°E) and one at Kilpisjärvi (69.0°N, 20.8°E) in northern Scandinavia, close to the magnetic footprint of GEOS-2. Time intervals between two successive frames is 20 s. An intense surge (Surge I) first appears in the central part of the figure, between 20.17.43 and 20.18 UT, and later propagates to the west. Other surges develop further to the north (Surges II and III). At 20.21, a well-defined surge develops in the same region as Surge I. It is not clear, however, that it propagates afterwards; hence, it is labelled DAF (Discrete Auroral Form) in what follows. In view of its very clear westward motion, Surge I is labelled WTS (Westward Travelling Surge) hereafter. Such a label is also consistent with the current idea that the WTS is the first surge to develop at breakup.

Figure 2 gives an overview of the various parameters measured at GEOS-2 over 1 hour. It shows the magnetic field in the VDH frame (V is radial outward, D is azimuthal and H is essentially parallel to the Earth's rotation axis, at GEOS orbit). Panel 2 shows the radial (E_R) and azymuthal (E_A) components of the electric field. The following panels show low energy and high energy particles. Let us describe the successive phases of the substorm.

The pre-substorm (before 20.17 UT) is characterized by a slow decrease of the H component of the magnetic field B accompanied by a slow increase of the V component until they reach comparable amplitudes, at 20.10 UT; accordingly, a "tail-like" configuration progressively builds up. Given the low magnetic latitude (~ 3°) of GEOS-2, the equality between the V and H components corresponds to a highly stressed magnetic field configuration, which is often observed for substorms developing in the pre-midnight sector at the geostationary orbit. The build-up of such a configuration implies an increase of the tail current and/or a motion of this current earthwards. Simultaneously, the radial component of the quasi-static electric field (E_R) progressively decreases, reaching -2mV.m⁻¹ at 20.15 UT. Hence, prior to the breakup, the electric field is radially earthward; the plasma motion ExB is directed azymuthally to the East.

The number density of low energy electrons (100-500 eV) is typical for the plasmasheet, thus indicating that, prior to the substorm breakup, GEOS was located within the plasmasheet.

The integral fluxes of energetic electrons (E > 22 keV) and ions (E > 27 keV) are plotted on the lowest panel. The ion flux progressively decreases until substorm breakup; the behavior of electrons is essentially the same but there is a



on

lded

two

e at

lose

vals

urge

gure,

o the

es II

same

at it

crete

clear

ward

istent

ge to

eters

netic

uthal

is, at

ruthal

anels

scribe

i by a

ield B

t until

UT;

builds

-2, the

ds to a

often

dnight

such a

nd/or a

ly, the

i (E_R) 15 UT.

adially

uthally

00 eV)

prior to

nin the

2 keV)

el. The

cup; the

ere is a

picture This defolded intensification between et al., 1991). one at Kilpisjärvi strong following surges (WTS (from Roux

GEOS-2, JANUARY 25, 1979

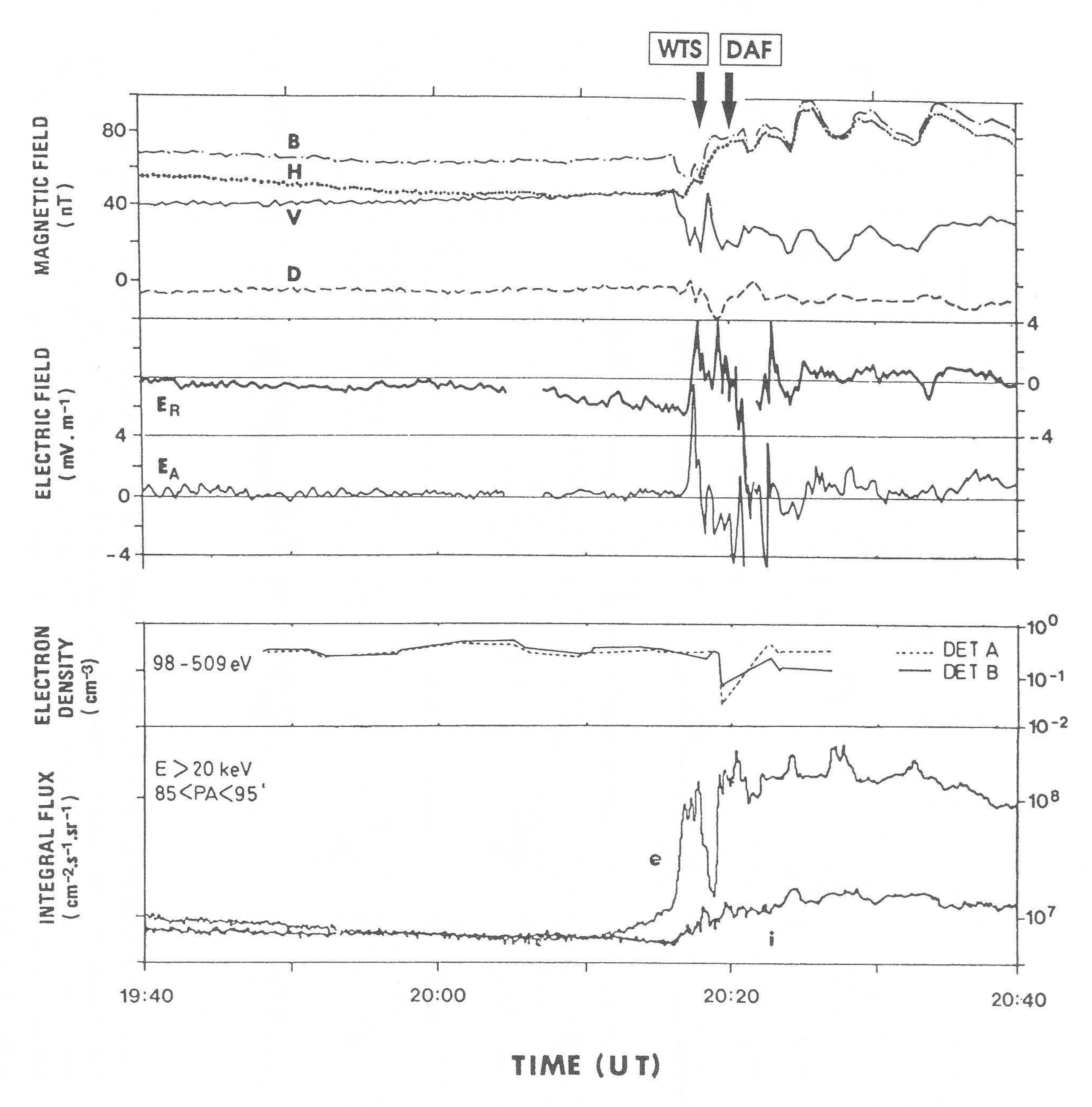


Fig. 2 (from Roux et al., 1991). Composite view showing one hour of data. From top to bottom: (i) the 3 components (VDH) of the magnetic field plus the total magnetic field (B), (ii) the radial and azymuthal component of the electric field, E_R and E_A , respectively, (iii) the electron density from detector A measuring perpendicular to the spin axis and B along the spin axis, and (iv) the integral flux of energetic electrons and ions above 20 keV for electrons and 27 keV for ions.

weak increase prior to the substorms. This increase is only observed, however, in the 2 lower energy channel (20-30 keV), as will be discussed later.

The active phase starts at 20.17 UT and lasts until 20.25; it is characterized by a sharp transition from a tail-like to a dipole-like configuration of the magnetic field. This transition is not monotonic; it is characterized by large fluctuations of the three components of the magnetic field. The total magnetic field (B) starts decreasing from 20.16 to 20.18 UT. Then, after 20.18 UT, it increases above its initial value. The first stage, i.e. the decrease of B, is associated with a decrease of the V component, H staying approximately constant. Later, after 20.18, the increase of B is due to an increase of the H component, V staying approximately constant, on average. Similarly, transient electric field spikes with very large amplitudes (E ≥ 10 mV.m⁻¹) are observed. During the active phase of the substorm, the number density of low energy electrons (> 500 eV) shows a deep minimum, as already pointed out by Shepherd et al. [1980]. Finally, the fluxes of both energetic electrons and ions suddenly rise up to values comparable to (for ions), or larger (for electrons) than the value they had well before the substorm. As noted by Sauvaud and Winckler [1980], the flux of energetic electrons is strongly correlated with the magnetic configuration; low fluxes correspond to tail-like and high fluxes to dipole-like configurations.

At the end of dipolarization, after 20.25, the dipolar configuration is established, since the H component is close to the total magnetic field B. Fluctuations of the magnetic field are still present but they now have longer periods and are more regular. These pulsations are predominantly compressional. B and the flux of energetic electrons are in antiphase. Low (E < 500 eV) and medium (0.5 < E < 20 keV) energy fluxes remain typical of the plasmasheet population; GEOS is still in the plasmasheet, but the magnetic configuration is more dipole-like, thus indicating that the tail current has been dissipated.

Figure 2 already gave evidence for a slow increase in the integral flux of electrons; this increase starts at ~ 20.00, about 20 mn before the breakup. Differential fluxes displayed in Figure 3 not only confirm this trend, but also indicate that it is limited to the lowest energy channels (essentially from 20 to 27 keV). At higher energies, the differential fluxes keep on decreasing slowly until the breakup. We believe this increase in the intensity of the lower energy channel is due to the inward motion of the plasmasheet and/or to its heating prior to the breakup. Such an interpretation is consistent with the model of Goertz and Smith [1989] who suggest that, prior to the breakup (that they attribute to a thermal catastrophe), the

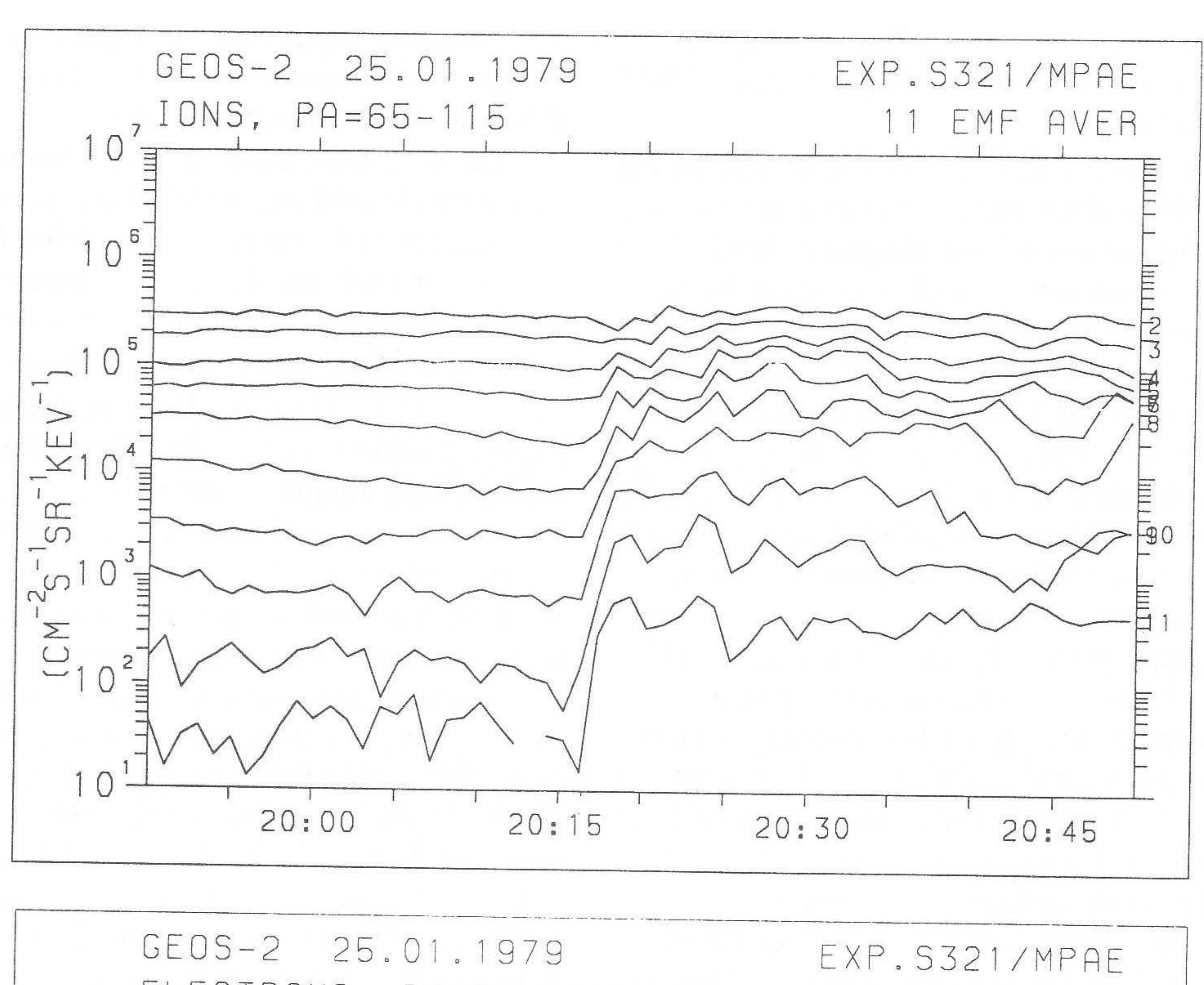
CPS is heated via resonant absorption of Alfven waves. An enhanced convection can also drive the plasmasheet earthward: there is indeed an increase in the modulus of the electric field, from 20.00 to 20.17, but this electric field is earthward-directed and not westward, as one would expect for an enhanced convection. This deviation from the westward direction is probably due to the location of the spacecraft, close to the Harang discontinuity, as evidenced by the radial electric field that builds up prior to breakup.

At ~ 20.17, differential fluxes start increasing in all energy channels, at the same time as the magnetic field configuration abruptly changes; this change is better seen in Figure 2, last panel, where the time resolution for the integral intensity is 5.5 s instead of 1 mn for Figure 3. At ~ 20.19, a second dispersionless increase of the electron intensity occurs in all energy channels.

Differential intensities of ions are displayed in Figure 3b. Here again, no significant energy dispersion can be measured; most of the energy channels show a peak at ~ 20.18. On the lowest energy channel (~ 27 keV), however, there is a decrease at 20.18 followed by two increases. This delay is not related to an energy dispersion; the observed transient oscillations in the flux of the lowest energy ions in Figure 3b are likely to be due to the development of the instability discussed in the rest of the paper. Time resolution, unfortunately, is not good enough on differential plots to ascertain this interpretation.

In summary, the study of the differential intensities of energetic electrons and ions leads to the identification of four time periods: (i) before 20.00 UT, in all energy channels, the differential intensities of energetic electrons and ions is constant or slowly decreasing, as the tail-like magnetic configuration builds up, (ii) from ~ 20.00 to ~ 20.17, the highly stressed tail-like configuration remains essentially the same, the intensities of the most energetic electrons and ions keep on decreasing slowly but the electron intensity at low energies increases, suggesting an heating of the plasmasheet, (iii) from 20.17 to ~ 20.20, dramatic increases in the intensities of electrons and ions occur. Differential intensities give evidence for transient oscillations, with a phase shift between electrons and ions, and some time lag between peaks at the lower and the higher energies, but no significant energy dispersion, and (iv) after 20.20, more regular oscillations of electrons and ions are observed, with little, if any, energy dispersion.

The main conclusion of this Section is that the dramatic increase observed at breakup in the differential intensities of energetic electrons and ions is not consistent with an energy dispersion. Roux et al. [1991] have shown that there is no pitch angle dispersion either (with a very high time resolution of 5.5 s). Then, energetic electrons and ions



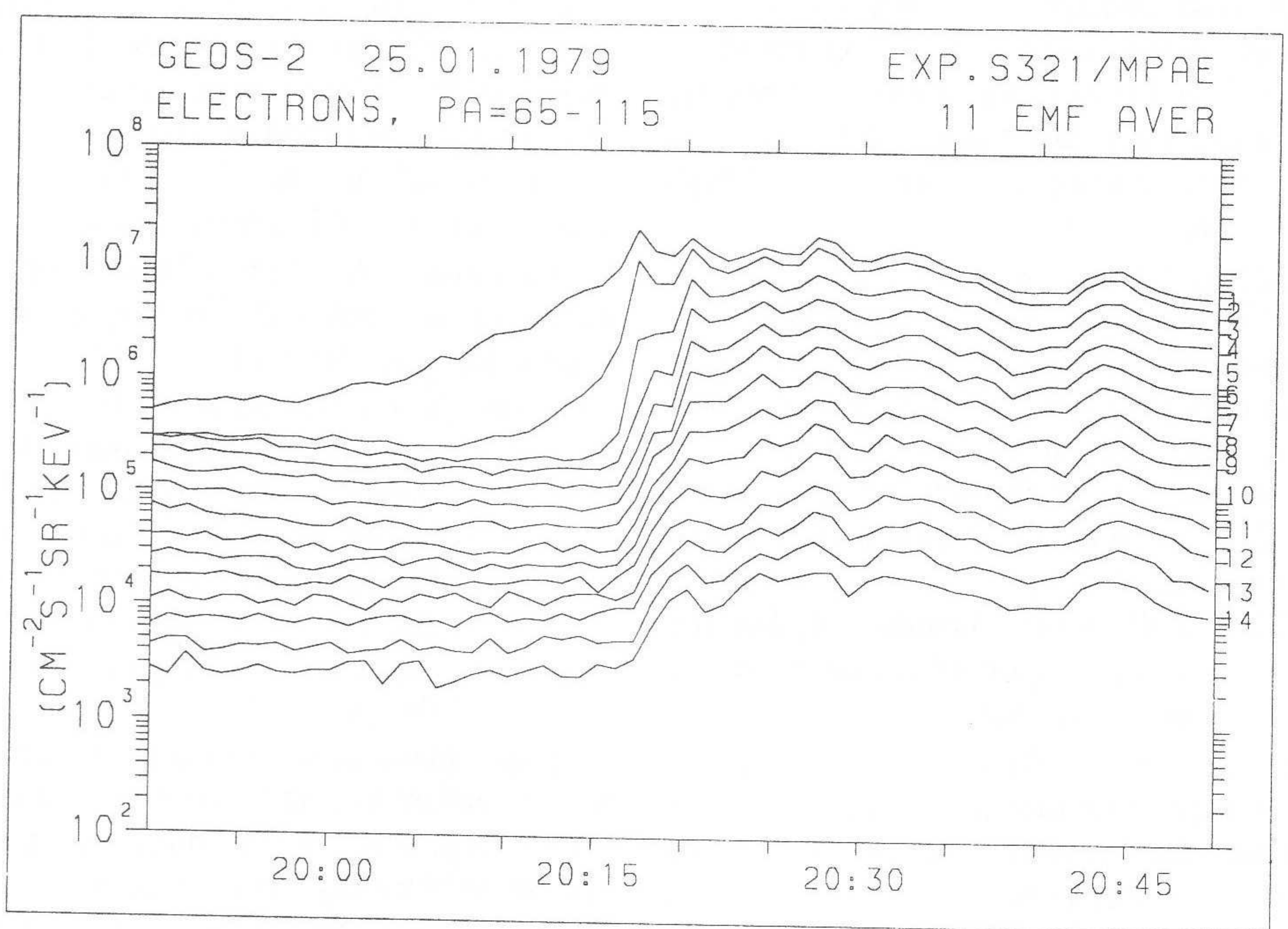


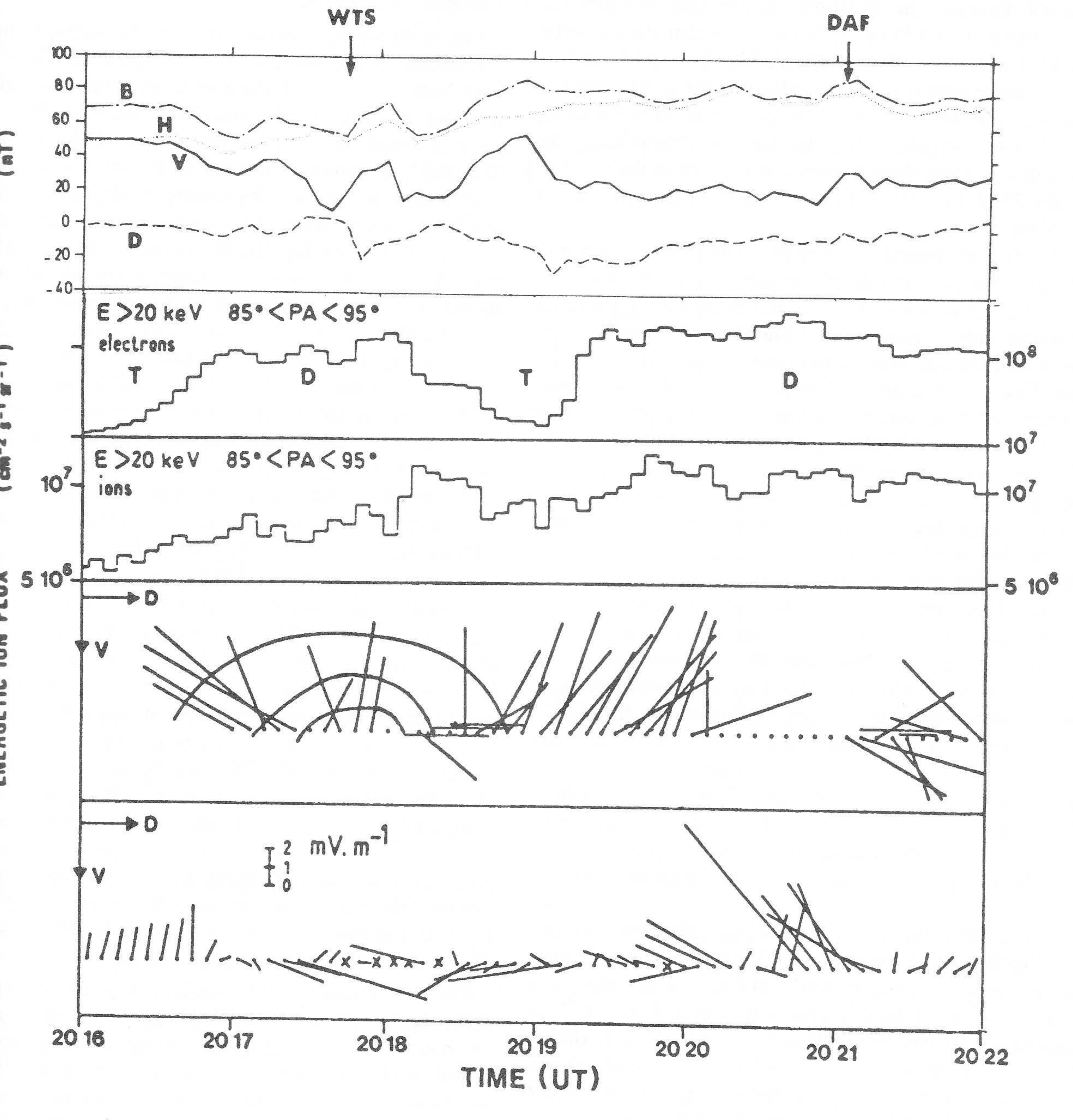
Fig. 3. Differential flux for energetic electrons (3a) and ions (3b), plotted over one hour, with ~ 1 mn time resolution. Notice that no clear energy dispersion shows up.

must have been accelerated locally or/and the spacecraft must have crossed a region with a sharp gradient in the intensities of energetic ions and electrons. Let us now use high time resolution measurements (5,5 s) to give evidence for the development of a ballooning instability.

3. BALLOONING INSTABILITY: EXPERIMENTA EVIDENCE

Most of the parameters displayed in Figure 4 are the sa as in Figure 2, but a higher time resolution is used: of

GEOS-2, JANUARY 25, 1979



ig. 4. Detailed composite figure showing (i) the magnetic field data in the VDH frame with 5.5 s resolution, (ii) ux of energetic electrons, (iii) flux of energetic ions, (iv) gradient in the flux of energetic ions, projected onto the D,D plane, and (v) direction of the spin-averaged electric field, also projected onto the V,D plane. Full lines on anel IV suggest the tentative isopressure contours; the size of the arrows is proportional to intensity of the radient in ions.

six minutes of data are displayed. Magnetic field data show large fluctuations, together with a change from a tail-like to a dipole-like configuration. The flux of energetic electrons (panel 2) is anti-correlated with the magnetic configuration; as BV decreases, the energetic electron flux increases and vice versa. T and D in the figure mean that the magnetic field is, in average, Tail- or Dipole-like. In panel 3, the flux of energetic ions is plotted. Notice that the scale is not the same as for electrons. While the general trend is the same, the flux of energetic ions is not really well correlated with that of electrons; there is even a maximum in the ion flux from 2018 to 2019 UT, whereas the electron flux is minimum.

The flux of energetic ions is not azimuthally symmetric. Because the Larmor radii of energetic ions are large (≥ 200 km), this asymmetry reflects the presence of a spatial gradient with a typical scale of a few Larmor radii. We have estimated the size and the direction of the gradients in the ion flux, as sketched in Figure 4, panel 4. The arrows indicate the direction and amplitude of the energetic ion flux gradient in the spin plane (roughly the V,D plane). Note that, on the average, the gradient is earthward, which suggests that the source of energetic ions is located earthward and not tailward, as is often assumed. This seems to be the more frequently encountered situation, as demonstrated in a companion paper by Korth et al. [this issue]. There are however significant departures from the earthward direction of the gradients; in particular the gradients just after 2018 and 2021 UT are eastwards. Tentative iso-contours of the flux have been plotted, whenever possible; they are perpendicular to the direction of the gradient in the ion flux. These changes in the direction of the gradient also suggest the existence of a wave-like structure passing by the spacecraft. This idea is supported by the good correlation existing between the variations of the magnetic configuration, the flux of energetic electrons and the changes in the direction of the gradient in the ion flux.

In the fifth panel of Figure 4, electric field vectors projected onto the spin plane (V,D) are plotted. These vectors have been determined from raw data, assuming that they are quasi-stationary over a spin period of 6 s. This assumption is certainly fulfilled before 2017 UT, that is before break up, where the E field was steady and directed earthwards. At break up the E field changes more quickly and the data shown here represent estimates. Clearly the size and direction of E change quite fast, especially around 2018 and 2021 UT when a WTS (WTS I) and a Discrete Auroral Form (DAF) are observed at GEOS 2 magnetic footprint. Crosses have been drawn instead of arrows, whenever the preamplifier of the E field experiment was saturated by too

large voltages. Intense E fields spikes are observed around 2018 and 2021 UT; at these times, there is a reversal in the direction of these spikes, from eastward to westward. Between these two times and later on, the electric field is essentially westwards.

Figure 4, panel 1, gives evidence for large, transient fluctuations in the magnetic field components. These data have been analysed with the help of the minimum variance analysis, applied to eight minutes of the data. This time interval comprises the most active part of the substorm. The result is shown at the top of Figure 5 where the 3 components B₁, B₂ and B₃ corresponding respectively to maximum, intermediate and minimum variance are plotted. The variances along B_1 , B_2 , B_3 directions are $\sigma_1 = 15$ nT, $\sigma_2 = 5.5 \text{ nT}$ and $\sigma_3 = 3.8 \text{ nT}$, respectively, for the sliding averaged data over 1 mn. For the 5.5 s resolution data, σ_1 = 15.5 nT, $\sigma_2 = 8.2$ nT and $\sigma_3 = 5.2$ nT. Minimum variance is essentially in the azimuthal direction, $\theta \sim 80^{\circ}$, $\phi \sim 92^{\circ}$, where θ and ϕ are the polar and azimuthal angles, measured with respect to the VDH frame of reference. Maximum variance is therefore essentially in a meridian plane, in a direction more or less perpendicular to the initial direction of the magnetic field. In the B2 component in particular, large amplitude, quasi periodic fluctuations are observed, with a pseudo period T of approximately 1 min.

In the lower left panel of Figure 5, an hodogram of the (sliding averaged) magnetic field is displayed, in the B₁, B₂ plane. For reference, the projection of B₁ B₂ plane on the V H plane is also sketched on the lower right panel (the angle between these planes is small but not zero). This hodogram gives evidence for a wave that is essentially polarized in the B₁, B₂ plane. The B₃ is not negligible, however. As discussed in Roux et al., 1991, the B₃ component which is along the D direction is indicative of field-aligned currents associated with the development of the instability (see Fig. 6). In addition to the signature of the wave which propagates azymuthally along the direction of minimum variance, there is a steady increase of the component along B₁, which is essentially perpendicular to the direction that the magnetic field had prior to the breakup.

Then minimum variance analysis applied to magnetic field data suggests azimuthally-propagating transient oscillations. Oscillations with the same pseudo-periods are found in (i) the direction of the gradient in the flux of energetic ions, (ii) the flux of energetic electrons, and (iii) the direction of the electric field. These observations suggest that an instability develops at breakup, in the near Earth plasmasheet. The observed gradient in the pressure of energetic ions is a clue to the identification of this instability. This gradient is, in average, directed earthwards, that is to say in the same direction as the gradient in the

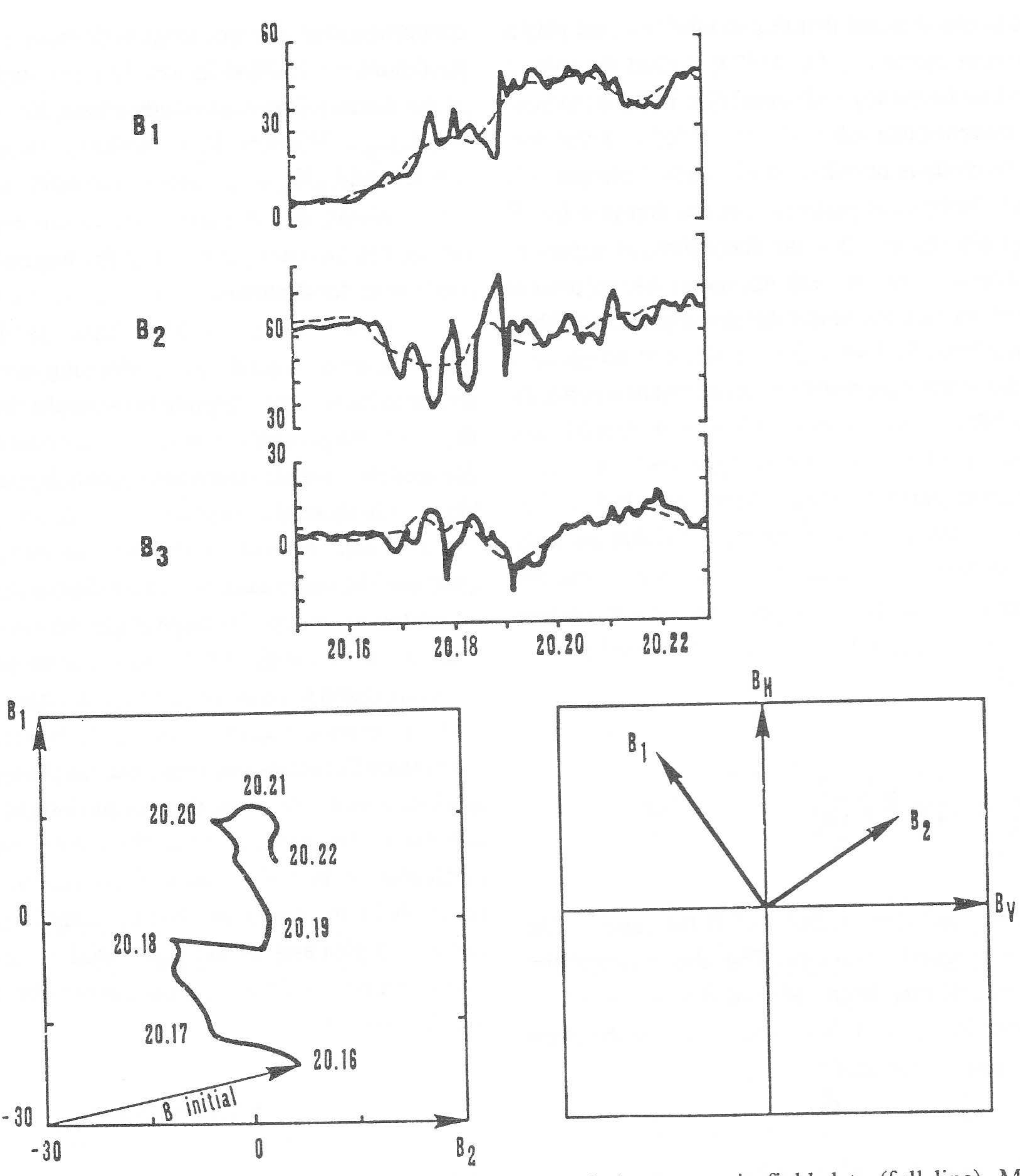


Fig. 5. Top: minimum variance analysis applied to 5.5 s resolution magnetic field data (full line). Maximum variance is for $\theta \sim 39^\circ$, $\phi = \sim 165^\circ$, minimum variance $\theta \sim 80^\circ$, $\phi \sim 92^\circ$). Dashed line corresponds to minimum variance applied to sliding averaged data; then maximum variance (B₁) corresponds to $\theta \sim 33^\circ$, $\phi \sim 164^\circ$ and minimum (B₃) variance to $\theta \sim 90^\circ$, $\phi \sim 106^\circ$. Bottom left: hodogram of sliding averaged data (B₁, B₂). Bottom right: projection of B₁B₂ in the VH frame. Amplitudes are $\sigma_1 \cong 15$ nT (maximum variance), $\sigma_2 \cong 5.5$ nT (mean), $\sigma_3 \cong 3.8$ nT (minimum).

magnetic field. This situation is known to be unstable to the ballooning modes. Korth et al. [this issue], show that earthward-directed pressure gradients, similar to these reported here, are indeed regularly observed at GEOS orbit, prior to breakup, at least for isolated dispersionless substorms.

4. BALLOONING INSTABILITY: THEORETICAL FRAMEWORK

The idea that an earthward-directed pressure gradient is unstable to interchange or ballooning modes is not new. Long ago, Swift [1967] suggested that the outer edge of the

ring current is unstable and that this instability could play a role in substorm dynamics. Liu [1970] studied the role of electrostatic low frequency drift instability in the behaviour of the ring current outer edge. He concluded that the drift flute $(k_{//} = 0)$ mode is unstable. In his study, however, Liu assumed that electrostatic perturbations develop in a low \beta $(\beta < m_e/m_i)$ plasma and that the ionosphere is a perfect conductor. These hypotheses are not applicable to present data; the perturbations are indeed electromagnetic and they take place in a large β plasma ($\beta \sim 1$). There is no obvious reason why the ionosphere could be considered as a perfectly conducting medium. More recently, Miura et al. [1989] have included finite \beta effects in their analysis and considered electromagnetic perturbations. They concluded that ballooning mode can be destabilized, provided that the scale of the pressure gradient (L_D) is small enough and that the perpendicular wave length is larger than the ion Larmor radius (ρ_i). These two conditions can be expressed as [see Roux et al., 1991]

$$\beta > \frac{L_p}{R_c} > \frac{\pi^2}{16} k_\perp^2 \rho_i^2$$
 (1)

where R_c is the curvature radius and β the ratio of the kinetic to the magnetic pressure. The above inegalities suggest that an arbitrary large value of β would meet the instability condition. In fact, β is constrained by the stress balance which can be expressed as

$$\frac{2L_{\mathbf{p}}}{R_{\mathbf{c}}} > \beta \tag{2}$$

Then

$$\frac{2L_{\mathbf{p}}}{R_{\mathbf{c}}} > \beta > \frac{L_{\mathbf{p}}}{R_{\mathbf{c}}} \tag{3}$$

A detailed comparison between the actual values of β, L_p, R_c, deduced from measurements made at substorm onsets, has been carried out by *Korth et al.* [this issue]. The

conclusion that emerges from their study is that the above conditions are fulfilled for the 22 cases studied. In the case of the January 25th event studied here, Korth et al. obtain $\beta \sim 2.1$, $L_p = 2950$ km, $R_c = 2480$ km. Then, $2L_p/L_c = 2.4$, $\beta = 2.1$ and $L_p/R_c = 1.2$; therefore condition (3) is satisfied.

Notice that the above values are not the measured values, but the ones projected at the magnetic equator [see *Korth et al.* for discussions].

Ohtani et al. [1989] have used the bi-fluid approximation to study the ballooning instability, which allows to include the coupling between the shear Alfven and the slow magnetosonic mode. The criteria that can be deduced from their study are essentially similar, but not identical to those given above.

Even the use of the bifluid approximation is questionable, under the extreme conditions that prevail prior to substorm breakup. The large angles between the measured magnetic field and the dipole field indicate that thin current sheets localized close to the geomagnetic equator, do develop prior to substorm breakup. Then, with such a thin layer, the ion bounce frequency can easily exceed the wave frequency. A kinetic description is then needed to account for the changes in the instability conditions along the field line. In particular, it is well known, from fusion devices, that reversals in the curvature that necessarily develop if the current is pinched in the equatorial region, do play a stabilizing role. All these effects can only be described by a kinetic analysis.

5. DISCUSSION

5.1. Consequences of the ballooning instability

While the diamagnetic current is divergence-free, the currents associated with gradient and curvature drift are not divergence-free, which leads to the generation of positive and negative charges at the leading and trailing edges of the azimuthally (here westward) propagating wave. Of course, the plasma does not support charge excesses, then field-aligned currents have to flow along field lines to maintain charge neutrality. This results in a bimodal field-aligned current system, with the current flowing successively towards the Earth, carried by upflowing electrons, and from the Earth, carried by precipitating electrons.

These precipitating electrons lead to the formation of the uroral structures (WTS and DAF) observed simultaneously on the ground. Then, the field-aligned current system, associated with the development of the ballooning astability, produces an upward current above the WTS, and sownward currents both to the west and to the east of the urge. This is indeed what Opgenoorth et al., [1983] and Cozelova and Lyatskiy [1984] have deduced from their measurements.

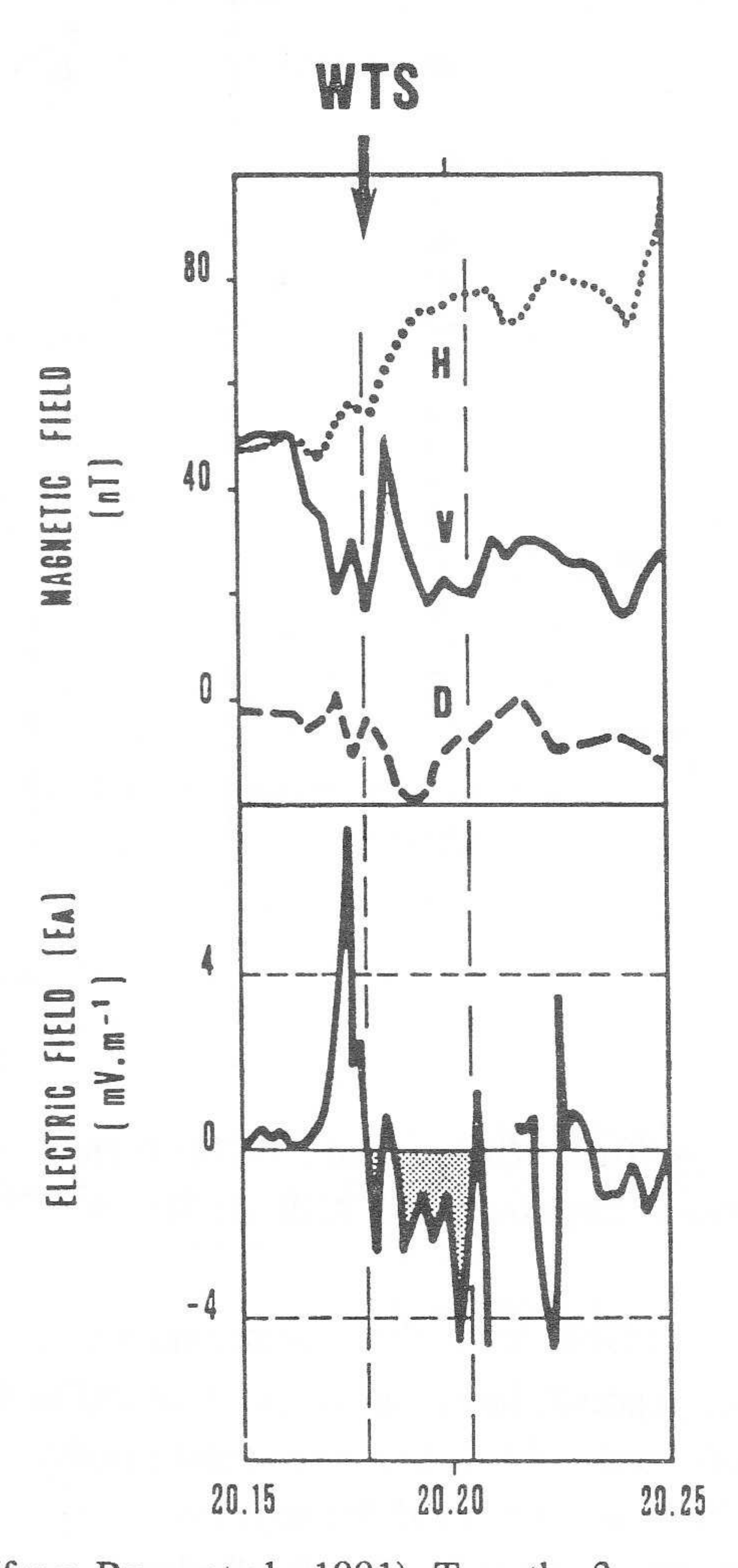
This field-aligned current system has to close, in the equatorial region and in the ionosphere. Figure 6 shows the first loop of this current system; the closure in the plasmasheet of the loop implies an eastward current, thereby leading to a reduction or even a cancellation of the tail current, at least locally. As suggested in Figure 6, this will result in an increase of the H component that tends to recover the dipole value. Such an increase produces an induced electric field oriented to the west. Figure 7 shows hat it is indeed the case; the increase of the H component does correspond to an enhanced westward electric field. Then, the dipolarization and the injection result from the current system imposed by the development of the ballooning instability.

NON LINEAR STAGE JIAIL

Fig. 6 (from Roux et al., 1991). Sketch showing the Fig. 7 (from Roux et al., 1991). Top: the 3 components of closure of the field-aligned current circuit and its effects on the reduction/cancellation of the tail current. Reduction in tail current implies $\partial B_H/\partial t > 0$ and hence an increase of the westward electric field.

5.2. Comparison with other observations

The idea that dispersionless injection can occur quite close to the Earth is not new; Mauk and McIlwain [1974] have already shown several examples of dispersionless injections of electrons and ions at substorm breakup, that they also interpret as a local injection process. Mauk and Meng [1987] have suggested that this injection mechanism is different from the mechanism of X line formation further out in the tail. Roux [1985] suggested that the injection at substorm could be due to an instability developing in the near Earth plasmasheet. Analyzing AMPTE CCE data,



the magnetic field in a VDH frame. Notice the increase of the H component. Bottom: azymuthal component of the electric field. The shaded area corresponds to the period where the H component drastically increases.

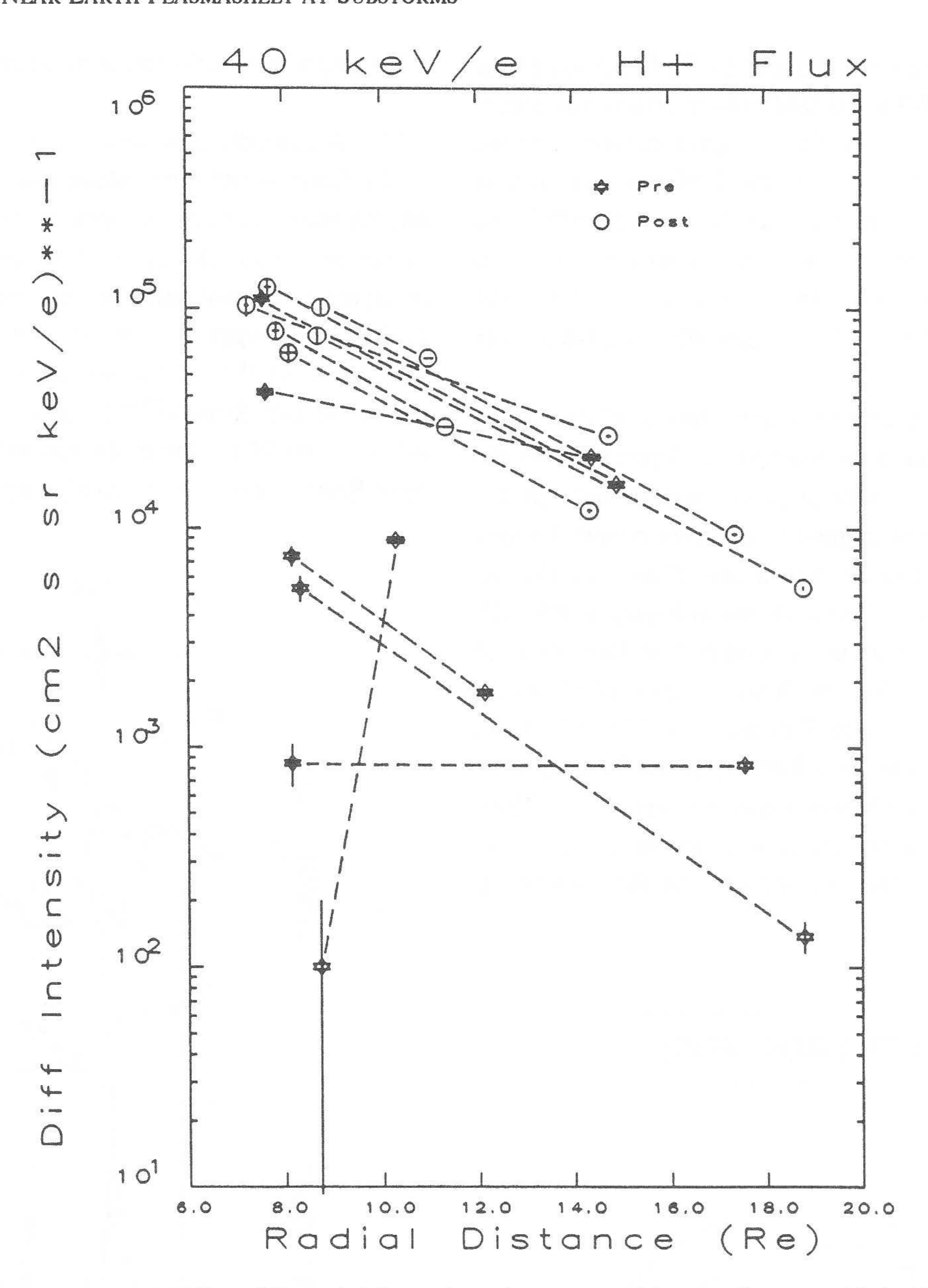


Fig. 8 (from Kistler et al., 1990). Differential intensity of protons with energies E > 40 keV/e versus radial distance. Data from both AMPTE IRM and CCE have been used to build this figure.

Lopez et al. [1988] found that dipolarization events, similar to the one reported here, can occur at all radial distances between 6.4 and ~ 9 R_E. In a more recent study, Lopez et al., [1990], have analyzed the azymuthal asymmetry of energetic ions, at breakup. Results displayed in plate 3 of their paper, for instance, can be interpreted as evidence for for a strong gradient in the ion pressure pointing successely earthward and tailward. Then these authors also found that the dipolarization of the magnetic configuration is directly

linked to oscillations in the direction of the ion pressure gradient. For a more detailed account of these results, see Lui [1991, this issue]. Kistler et al. [1990] have combined data from AMPTE IRM and CCE when these spacecraft were located in the night sector at different radial distances, but at similar longitudes. Kistler et al. have shown that the ion bursts observed at substorm breakup had very similar spectra at both locations. Post-injection fluxes at energies 40 keV were found to depend only on radial distances, and

the same composition ratios O⁺/H⁺ and He⁺⁺/H⁺ were found at both locations.

Figure 8, taken from Kistler et al. [1990], shows the prefluxes (stars) and the post breakup fluxes (circles) These fluxes are measured between ~ 7 and - 19 R_F by AMPTE IRM and CCE. While the prefluxes are at random, the post breakup fluxes are and organized by the radial distance and show coherent the two spacecraft locations. These data are not consistent with ions being accelerated in a given region: the plasmasheet or the inner plasmasheet, and convected afterwards, to the observation point. Instead, these data same acceleration process can be operative over a broad region in the tail. If the ballooning instability here is the process that leads to this energization then it should develop simultaneously over a broad of radial distances, or propagate quite fast across the plasmasheet.

In a recent paper, Jacquey et al. [1991] have used manetic field data from the ISEE spacecraft located in the ball lobes, to study the possible motion of dipolarization wents. They found that the dipolarization usually starts are close to the Earth, at 6-8 R_E, and later propagates or expands at ~ 300 km/s towards the tail. This analysis suggests then that the dipolarization that follows the current disruption propagates/expands tailwards at a very large velocity.

CONCLUSION

An alternative approach to the problem of the dissipation of magnetic energy stored in the geomagnetic tail has been proposed. It is based on the ballooning instability fed by strong earthward gradients in the flux of energetic ions. This instability, which does not require that the vertical component of the magnetic field goes to zero, can explain the dipolarization/injection occurring at breakup. If, as suggested by *Jacquey et al.* [1991], the dipolarization events first develop at R ~ 6-8 R_E and later propagate or expand tailwards at a large velocity, then the northward motion or expansion of the arcs are the natural consequence of the motion/expansion of the instability that lead to the depolarization.

Acknowledgements. We acknowledge helpful discussions with D. Le Quéau, S. Ohtani, R. Pellat, and R. Tamao.

REFERENCES

Dungey, J.W.., Interplanetary magnetic field and the auroral zones, *Phys. Rev. Lett.*, 6, 47, 1961.

Goertz, C.K., and R.A. Smith, The thermal catastrophe model of substorms, J. Geophys. Res., 94, 6581, 1989.

Jacquey, C., J.A. Sauvaud, and J. Dandouras, Location and propagation of the magnetotail current disruption during substorm expansion: analysis and simulation of an ISEE multi-onset event, *Geophys. Res. Lett.*, 18, 389, 1991.

Kistler, L.M., E. Möbius, B. Klecker, D. Hovestadt, G. Glöcker, F.M. Ipavitch, and D.C. Hamilton, Spatial variations in the suprathermal ion distributions during substorms in the plasmasheet, *J. Geophys. Res.*, submitted to, 1990.

Korth, A., Z.Y Pu, G. Kremser, and A. Roux, A statistical study of substorm onset conditions at geostationary orbit, this issue, 1991.

Kozelova, T.V., and V.B. Liatskiy, A longitudinal current in front of a westward travelling surge, *Geomagn. and Aeron.*, 24, 191, 1984.

Lembège, B., and R. Pellat, Stability of a two-dimensional quasineutral sheet, *Phys. Fluids*, 25, 1995, 1982.

Liu, C.S., Low frequency drift instabilities of the ring current belt, J. Geophys. Res., 75, 3789, 1970.

Lopez, R.E., D.G. Sibeck, A.Y.T. Lui, K. Takahashi, R.W. McEntire, T.A. Potemra, and D. Klumpar, Substorm variations in the magnitude of the magnetic field: AMPTE/CCE observations, J. Geophys. Res., 53, 14,444, 1988.

Lopez, R.E., H. Lühr, B.J. Anderson, P.T. Newell, and R.W. McEntire, Multipoint observations of a small substorm, J. Geophys. Res., 95, 18,897, 1990.

McPherron, R.L., C.T. Russell, and M.P. Aubry, Satellite studies of magnetospheric substorms on August 15, 1968. Phenomenological model for substorms, *J. Geophys. Res.*, 78, 3131, 1973.

Mauk, B.H., and C.E. McIlwain, Correlation of k_p with the substorm-injected plasma boundary, *J. Geophys. Res.*, 79, 3193, 1974.

Mauk, B.H., and C.I. Meng, Plasma injection during substorms, *Physica Scripta*, *T-18*, 128, 1987.

Miura, A. S. Ohtani, and T. Tamao, Ballooning instability and structure of diamagnetic hydromagnetic waves in a model magnetosphere, *J. Geophys. Res.*, 94, 231, 1989.

sure see ined raft ces, the ilar gies

and

Ohtani, S., A. Miura, and T. Tamao, Coupling between Alfven and slow magnetosonic waves in an inhomogeneous finite-b plasma. Coupled equations and physical mechanism, *Planet. Space Sci.*, 37, 567, 1989.

Opgenoorth, H.J., R.J. Pellinen, W. Baumjohann, E. Nielsen, G. Marklund, and L. Eliasson, Three-dimensional current flow and particle precipitation in a westward travelling surge (observed during the BA-GEOS experiment), J. Geophys. Res., 88, 3138, 1983.

Pellat, R. Une nouvelle approche de la reconnexion magnétique : sous-orages magnétiques et vent stellaires, C.R. Acad. Sci., to be published, 1991.

Roux, A., Generation of field-aligned current structures at substorm onset, ESA SP-235, 151, 1985.

Roux, A., S. Perraut, P. Robert, A. Morane, A. Pedersen, A. Korth, G. Kremser, B. Aparicio, D. Rodgers, and R.

Pellinen, Plasma instability related to the westward travelling surge, J. Geophys. Res., to be published, 1991. Sauvaud, J.A., and J.R. Winckler, Dynamics of plasma energetic particles and fields near geosynchronous orbit in the night-time sector during magnetospheric substorms,

J. Geophys. Res., 85, 2043, 1980.

Shepherd, G.G., R. Boström, H. Derblom, C.G. Fälthammar, R. Gendrin, K. Kaila, A. Korth, A. Pedersen, R. Pellinen, and G.L. Wrenn, Plasma and field signatures of poleward propagating auroral precipitation observed at the foot of the GEOS 2 field line, *J. Geophys. Res.*, 85, 4587, 1980.

Swift, D.W., The possible relationship between the auroral breakup and the interchange instability of the ring current, *Planet. Space Sci.*, 15, 1225, 1967.